A Novel Fault-Location Algorithm for Long Transmission Lines Compensated by Series FACTS Devices

Mahdi Ghazizadeh Ahsaee and Javad Sadeh, *Member, IEEE*

***Abstract*—This paper introduces a new noniterative fault-location algorithm for long transmission lines compensated by a series flexible ac transmission systems (FACTS) device. In the proposed algorithm, synchronous voltage and current samples from both ends of the transmission line are used and the distributed parameter line model in the time domain is applied. Due to the difficulties in the modeling of the series FACTS devices during a fault, the presented method does not use the model of the series devices. In this paper, the fault-location problem is converted to an optimization one in which the location and resistance of the fault are the decision variables. The proposed method includes three stages. Two fault locations are obtained, corresponding to the first two stages. In stage three, the obtained results from stages 1 and 2 are compared, and the correct fault location is selected. The proposed algorithm is a noniterative one and it is suitable for transmission lines compensated by any series FACTS device which could have the overvoltage protection and can be in any operating mode. The performance of the proposed algorithm is evaluated under different structural and fault conditions. The simulation results confirm the accuracy of the proposed algorithm.**

***Index Terms*—Distributed parameter line model, fault location, series flexible ac transmission systems (FACTS) device, synchronous sampling, time domain.**

I. Introduction

THE development of accurate fault-location techniques is very important, especially for the long transmission lines in arduous and rough terrain, to reduce the repair expense and speed up the restoration of service for power utilities and, consequently, to greatly improve the reliability of the system.

Series compensations have been successfully used to enhance the system stability and Increase loadability of high-voltage transmission lines. So far, different algorithms have been proposed for locating the faults on the series-compensated transmission lines [1]–[6] that use the data of one terminal [1], [2] and the data of two terminals [3]–[6]. In some of the algorithms, the phasor of measured voltages and currents are used [1], [5] that need to filter to obtain the fundamental frequency of voltages and currents. Generally, the frequency response of the filter and dc component of the transient signals could produce errors in results. A solution for this difficulty is to utilize the samples of the voltages and currents in the time domain [3], [4], [6]. Some of the algorithms [3], [5], [6] use the partial differential equations of the transmission-line model which accurately model the line and are suitable for long transmission lines. Thus, for more accuracy, the partial differential equations in the time domain are applied for modeling the line, in the presented method.

From the other point of view, fault-location algorithms for transmission lines compensated by the series devices can be classified into two groups. The first group utilizes the model of the series compensation [1], [3], [4] and includes inherent errors depending on the model of the series compensation, since during faults:

- the series device could change its operating mode [7] which is dependent on the protection, control strategies, and steady-state operating condition before the fault occurrence; so it is difficult to specify the mode that the series device transits to it;
- the series device does not change its mode instantly and it is not possible to accurately estimate the instants that the series device commences and finishes when changing its mode of operation.

With the aim of overcoming such difficulties, in the second group of algorithms [5], [6], the compensator model is not used. Thus, the errors corresponding to the modeling of the series compensator are removed. In [5], a phasor measurement unit (PMU)-based scheme is proposed which is an iterative fault-location method. The partial differential equations of the transmission line in the time domain are used in [6] which is also iterative. In the first iteration, the voltage drop across the series compensator is ignored and an initial solution for the location of fault is calculated. In the other iterations, the voltage of the series compensator is calculated, and updated using the obtained location of the fault in the previous iteration. The procedure is repeated until the convergence is achieved. The calculations are executed iteratively, in [5] and [6]. To execute iterative calculations, the initial values for the sought unknowns have to be chosen on which the convergence of these algorithms depends. The other difficulty with such calculations appears when no unique solution for the unknowns is possible. Performing iterative calculations, the valid solution may not be the result [8].

The fault-location algorithm proposed in this paper differs from the presented approaches in [5] and [6]. The difference relies on that the presented algorithm here avoids iterative calculations and does not need to calculate and use the voltage drop across the series compensator iteratively.

Manuscript received August 18, 2010; revised July 16, 2011; accepted August 18, 2011. Date of current version October 07, 2011. Paper no. TPWRD-00623-2010.

The authors are with the Electrical Engineering Department, Faculty of Engineering, Ferdowsi University of Mashhad, Mashhad, Iran (e-mail: mahdi_ghazy@yahoo.com; sadeh@ieee.org).

Color versions of one or more of the figures in this paper are available online at http://ieeexplore.ieee.org.

Digital Object Identifier 10.1109/TPWRD.2011.2166410

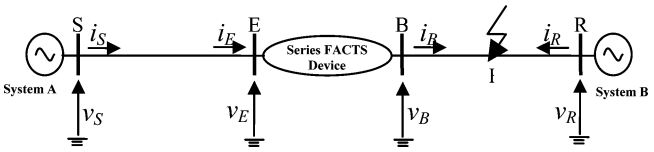

Fig. 1. Series-compensated transmission line with a fault on the right-hand side of the compensator.

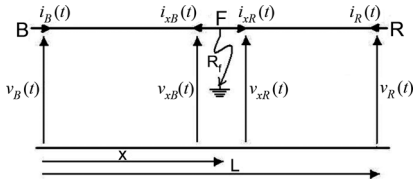

Fig. 2. Second part of the transmission line (section BR) with distributed parameters.

In this paper, a noniterative fault-location algorithm for long transmission lines compensated by a series flexible ac transmission systems (FACTS) device has been introduced. This technique does not use the model of the series device, because of the difficulties in the modeling of the series FACTS devices during the faults. In this algorithm, synchronized voltage and current samples from both ends of the transmission line and distributed parameter line model in the time domain are utilized. The method includes three stages. In the first and second stages, it is assumed that the fault is located on the right- and left-hand side of the series compensator, respectively. Two locations of faults corresponding to each stage are calculated. However, one of them is correct. In stage 3, the results obtained from stages 1 and 2 are compared, and the correct location of the fault is selected. The proposed fault-location algorithm does not need to calculate and use the voltage drop of the series compensator iteratively and the algorithm avoids iterative calculations. A 300-km, 500-kV transmission line compensated by the thyristor-controlled switched capacitor (TCSC) has been used to evaluate the accuracy of the proposed algorithm. The accuracy of the proposed method is very high and the average absolute error is about 0.0625%, without considering measurement and synchronization errors.

The rest of this paper is organized as follows. Section II explains the principal of the proposed fault-location algorithm for the series-compensated long transmission lines. In Section III, the results of the Matlab/Power System Blockset simulation-based evaluation of the developed fault-location algorithm are presented and discussed. The evaluation is followed by the conclusion in Section IV.

II. Principle of the Proposed Method

Fig. 1 shows a series-compensated three-phase transmission line in which a symmetrical three-phase fault has taken place on the right-hand side of the compensator. In this figure, S and R represent the sending and receiving ends of the line, respectively. In the proposed algorithm, synchronous voltage and current samples from both ends of the transmission line have been used. The current at the left-hand side of the series FACTS device (i_E) can be calculated using the sending-end recorded data of the voltage and current (v_S, i_S). The current at the right-hand side of the series FACTS device (i_B) is equal to i_E, so i_B is known.

On the other hand, the receiving-end voltage and current are available. Therefore, for the section BR of the line, the current of bus $B(i_B)$ and the voltage and current of bus $\mathrm{R}(v_R, i_R)$ are known and the voltage of bus $\mathrm{B}(v_B)$ is unknown. Having known information, it is not possible to use the conventional two-terminal fault-location algorithms, which are presented in the related literature. The same condition is considered when a fault takes place on the left-hand side of the compensator. A solution to overcome this difficulty is to estimate the voltage of bus B and to use it for conventional two-terminal fault-location algorithms. In this case, the model of the compensator and its operating mode are needed, but in this paper, a new algorithm is proposed in which the known data (v_R, i_R, and i_B) are used and are sufficient to find the location of the fault, and estimation of the voltage of bus $\mathrm{B}(v_B)$ is not needed.

In the following text, at first, the basic principle of the proposed algorithm is illustrated based on the known data for the section BR of the line considering a symmetrical three-phase fault and using the distributed parameter line model. Then, it is extended to consider the case of unsymmetrical faults.

A. Symmetrical Three-Phase Fault Case in the Transmission Line Without Series Compensation

A single-phase model of the part BR of the transmission line is shown in Fig. 2. The line length is L. F is taken as an arbitrary point at a distance x from bus B along the line and a fault has occurred at this point and the fault resistance is assumed to be R_f. As mentioned previously, it is assumed that $v_R(t)$, $i_R(t)$, and $i_B(t)$ are known and available for a predetermined period of time during the fault and $v_B(t)$ is unknown.

Based on Fig. 2, the voltage and current at the right-hand side of the fault point $(v_{xR}(t), i_{xR}(t))$ can be calculated using the receiving-end voltage and current [3] as shown in (1) and (2), at the bottom of the next page, where

τ	elapsed time for the wave propagation from B to F;
T_R	elapsed time for the wave propagation from B to R;
Z_c	characteristic impedance;
R'_R	line resistance from R to F, and we define

$$R'_{Rc} = Z_c + \frac{R'_R}{4},\ R''_{Rc} = Z_c - \frac{R'_R}{4}.$$

Also, (3), shown at the bottom of the next page, can be written for $i_B(t)$ [3], where

$v_{xB}(t), i_{xB}(t)$	voltage and current at the left hand-side of the fault;
R'_B	line resistance from B to F

$$R'_{Bc} = Z_c + \frac{R'_B}{4},\ R''_{Bc} = Z_c - \frac{R'_B}{4}.$$

Due to the continuity of the line and, therefore, the continuity of the voltage along the line, the following equation can be written:

$$v_{xB}(t) = v_{xR}(t). \tag{4}$$

At the fault point, using Circuit's law, this relation can be obtained

$$i_{xB}(t) = -i_{xR}(t) - \frac{v_{xR}(t)}{R_f}. \tag{5}$$

By substituting (4) and (5) into (3)

$$i_B(t) = \frac{\left(\begin{array}{l} R'_{Bc}\left[\left(1+\frac{R'_{Bc}}{R_f}\right).v_{xR}(t+\tau) + R'_{Bc}i_{xR}(t+\tau)\right] \\ -R''_{Bc}\left[\left(1-\frac{R''_{Bc}}{R_f}\right).v_{xR}(t-\tau) - R''_{Bc}i_{xR}(t-\tau)\right] \\ -\frac{R'_B}{4}.\left[\left(2+\frac{R'_B}{2.R_f}\right).v_{xR}(t) + \frac{R'_B}{2}i_{xR}(t)\right] \end{array}\right)}{2Z_c^2.} \tag{6}$$

Also, by substituting (1) and (2) into (6), the current at bus $B(i_B(t))$ is obtained as a function of the voltage and current of the receiving end (v_R, i_R), the elapsed time for the wave propagation from B to F (τ), and the fault resistance (R_f) as follows:

$$i_B(t) = f_1(v_R, i_R, t, \tau, R_f). \tag{7}$$

As mentioned before, it is assumed that $v_R(t)$, $i_R(t)$, and $i_B(t)$ are available. So the following equation can be written based on (7):

$$F(i_B, v_R, i_R, t, \tau, R_f) = 0. \tag{8}$$

In this equation, there are two unknown quantities τ and R_f. τ is proportional to the fault distance from $\mathrm{B}(x)$, so after calculating τ, the fault distance is determined. To obtain τ and R_f, at first nonlinear (8) is discretized

$$F(i_B, v_R, i_R, k, m, R_f) = 0 \tag{9}$$

where

$m.\Delta t = \tau$

$k.\Delta t = t$

Δt sampling step;

k, m arbitrary integers.

The samples of the voltage and current of bus R and the current samples of bus B should satisfy this discretized equation; thus, the fault-location problem can be converted to an optimization one as

$$\begin{cases} \mathrm{Min}\, J(m, R_f) = \underset{m,R_f}{\mathrm{Min}} \sum F^2(i_B, v_R, i_R, k, m, R_f) \\ \quad \mathrm{Subject\ to}: 0 \le R_f \\ \qquad\qquad 0 < m < m_{\max R} \end{cases} \tag{10}$$

where

$m_{\max R}.\Delta t = T_R.$

The optimization problem should be solved considering two constraints. Since the fault resistance is a positive value, the constraint $R_f \ge 0$ is added to the optimization problem. Also, this problem should be solved along the line, and L is proportional to T_R; therefore, $0 < m < m_{\max R}$. Since m is limited between 0 and $m_{\max R}$, this optimization problem can be solved by using the enumeration method. Thus, the objective function values should be calculated for all m between 0 and $m_{\max R}$, then the problem can be solved by choosing the minimum of the objective function values. So, set m to 1, since (9) has one unknown quantity (i.e., R_f), using the least-square estimation method, R_f is calculated, and is named R_{f1} after that the objective function value $J(1, R_{f1})$ is obtained. Then, by increasing m to 2, R_{f2} is achieved from (9) and the objective function value $J(2, R_{f2})$ is also the result. This procedure is continued for all m. Therefore, the objective function values for all m between

---

$$v_{xR}(t) = \frac{\left(\begin{array}{l} R'^2_{Rc}[v_R(t+T_R-\tau) - R'_{Rc}i_R(t+T_R-\tau)] + R''^2_{Rc}[v_R(t-T_R+\tau) + R''_{Rc}i_R(t-T_R+\tau)] \\ -\frac{R'_{Rc}R'_R}{4}.\left[\frac{\frac{R'_R}{2}}{R'_{Rc}}.v_R(t) + 2R''_{Rc}i_R(t)\right] \end{array}\right)}{2Z_c^2} \tag{1}$$

$$i_{xR}(t) = \frac{\left(R'_{Rc}[v_R(t+T_R-\tau) - R'_{Rc}i_R(t+T_R-\tau)] - R''_{Rc}[v_R(t-T_R+\tau) + R''_{Rc}i_R(t-T_R+\tau)] - \frac{R'_R}{4}.\left[2v_R(t) - \frac{R'_R}{2}i_R(t)\right]\right)}{2Z_c^2} \tag{2}$$

$$i_B(t) = \frac{\left(R'_{Bc}[v_{xB}(t+\tau) - R'_{Bc}i_{xB}(t+\tau)] - R''_{Bc}[v_{xB}(t-\tau) + R''_{Bc}i_{xB}(t-\tau)] - \frac{R'_B}{4}.[2v_{xB}(t) - \frac{R'_B}{2}i_{xB}(t)]\right)}{2Z_c^2} \tag{3}$$

0 and $m_{\max R}$ are determined, and the solution of the optimization problem can be obtained by choosing the minimum of these objective function values.

B. Symmetrical Three-Phase Fault Case in the Series-Compensated Transmission Line

Since the fault location with respect to the series compensator is unknown prior to fault-location estimation, at first, the proposed algorithm calculates two locations of fault via stages 1 and 2. In stage one, it is assumed that the fault is located on the right hand-side of the series compensator and in the second stage, the fault is assumed to be located on the left-hand side of the series compensator. The proposed method in two stages is the same but with different data. Finally, a comparing procedure is utilized to select the correct solution in stage 3.

1) Stage One: Consider Fig. 1 that shows a series-compensated three-phase transmission line in which a symmetrical three-phase fault has occurred on the right hand-side of the compensator. As mentioned previously, the current at the left-hand side of the series FACTS device ($i_E(t)$) can be obtained as a function of the sending-end voltage and current (v_S, i_S). The current at the right-hand side of the series FACTS device $i_B(t)$ is equal to $i_E(i)$, so

$$i_B(t) = f_2(v_S, i_S, t). \tag{11}$$

Considering the line BR, the current of bus B (i_B) can be calculated by using (11) and the voltage and current of R are available; therefore, the optimization problem (10) can be utilized. After discretizing (11) and by substituting it into (10), the following optimization problem is obtained:

$$\begin{cases} \text{Min } J_R(m, R_f) = \underset{m,R_f}{\text{Min}} \sum F_1^2(v_S, i_S, v_R, i_R, k, m, R_f) \\ \quad \text{Subject to:} \quad R_f \geq 0 \\ \qquad\qquad\quad 0 < m < m_{\max R}. \end{cases} \tag{12}$$

Solving (12) by using the enumeration method, the first stage offers the solution (J_R^*, x_R, R_{fR}) assuming the fault on the right-hand side of the series FACTS device. x_R and R_{fR} are the location and resistance of the fault, respectively, and J_R^* is the optimum value of the objective function according to x_R and R_{fR}.

2) Stage Two: In this stage, it is assumed that the fault has occurred on the left-hand side of the series compensator and the line BR is not defected. So the current at the right-hand side of the series FACTS device (i_B) can be derived as a function of the receiving-end voltage and current (v_R, i_R). $i_E(t)$ is equal to $i_B(t)$; thus, $i_E(t)$ and the voltage and current of bus S are known and available for the line SE, and the proposed procedure presented in Section II-A. can be used. For this case, the optimization problem will be

$$\begin{cases} \text{Min } J_S(m, R_f) = \underset{m,R_f}{\text{Min}} \sum F_2^2(v_S, i_S, v_R, i_R, k, m, R_f) \\ \quad \text{Subject to:} \quad R_f \geq 0 \\ \qquad\qquad\quad 0 < m < m_{\max S} \end{cases} \tag{13}$$

where

$m_{\max S}.\Delta t = T_S$

T_S elapsed time for the wave propagation from S to E.

Solving the above optimization problem, using the same algorithm as the previous stage, x_S and R_{fS} are calculated, which are the location and resistance of the fault, respectively. So the second stage results in the solution (J_S^*, x_S, R_{fS}) assuming the fault on the left-hand side of the series compensator and J_S^* is the optimum value of the objective function J_S, according to x_S and R_{fS}.

3) Stage Three; Selecting the Correct Solution: A simple and straightforward algorithm to select the correct side of the fault was presented in [1]. In this paper, a new algorithm is proposed to select the correct fault side using the objective function values. This algorithm selects one of the two solutions calculated from the first stage (J_R^*, x_R, R_{fR}) and the second stage (J_S^*, x_S, R_{fS}) according to the following descriptions and then the correct location of the fault is identified.

As mentioned previously, it is assumed that a symmetrical three-phase fault has occurred at one point of the transmission line, and this point is located on one of the two sides of the compensator; thus, the fault point is unique. The objective function J_R is valid only for the right-hand side of the compensator and is not valid for the left-hand side of it and this is converse for J_S. Therefore, one of the two optimization problems derived in stages 1 and 2 is valid for the true fault point, and results in minimum value. So, one of the two values J_R^* and J_S^* with respect to the true location of fault has the least value. Thus, the fault side is identified after finding the minimum value of the two solutions (J_R^* and J_S^*)

$$J^* = \text{Min}(J_R^*, J_S^*). \tag{14}$$

Then, the location of fault with respect to the minimum of J_R^* and J_S^* is the correct one.

The flowchart of the proposed fault-location method is shown in Fig. 3. At first, the voltages and currents of both ends of the transmission line are measured synchronously and transmitted to the fault locator point. As explained previously, the fault-location algorithm contains three stages. In stage one, it is assumed that the fault is located on the right-hand side of the compensator, and the obtained optimization problem (12) is solved by using the enumeration method, and the solution (J_R^*, x_R, R_{fR}) is calculated. Stage two is the same as e stage one, but with different data, and the solution (J_S^*, x_S, R_{fS}) is obtained. In stage three, the minimum of two solutions (J_R^* and J_S^*) is calculated (J^*), and the location of fault corresponding to J^* is selected as the correct one.

As seen from stages 1 and 2, the derived optimization problems need only the sending- and receiving-end recorded data to solve and find the location of fault, and there is not any relation to the model of the series compensator. In addition, this method does not need initial values and iterative calculations. Therefore, the salient advantages of the proposed algorithm are that the method is a noniterative one and it does not need to have any knowledge from the series compensator model, its control system parameters, and operating mode.

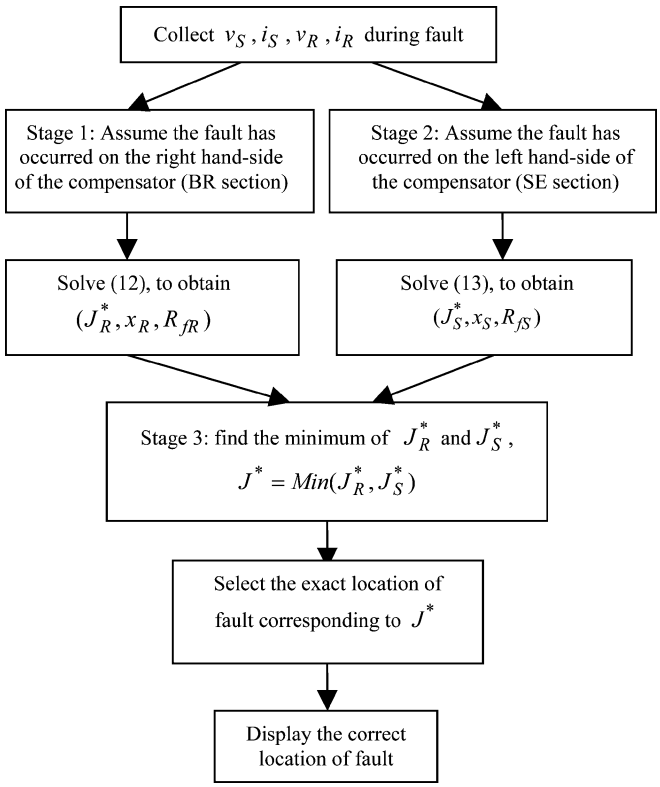

Fig. 3. Flowchart of the proposed fault-location method.

C. Applying the Proposed Method for Locating Unsymmetrical Faults

In a three-phase transmission line, the voltages and the currents of the line are related to self and mutual coupling distributed parameters of the phases that this relation is expressed by partial differential equations [9]:

$$\begin{cases} \frac{\partial \mathbf{v}}{\partial x} = -\mathbf{L}\frac{\partial \mathbf{i}}{\partial t} - \mathbf{R}.\mathbf{i} \\ \frac{\partial \mathbf{i}}{\partial x} = -\mathbf{C}\frac{\partial \mathbf{v}}{\partial t} \end{cases} \tag{15}$$

where $\mathbf{R}$, $\mathbf{L}$, and $\mathbf{C}$ are 3×3 resistance, inductance and capacitance matrices (in per-unit length of the line), respectively; and $\mathbf{v}$ and $\mathbf{i}$ are third-order column vectors representing voltages and currents. A transformation determined from a solution of the eigenvalue analysis can be used to decompose the partial differential equations into three modal components [9]. The following set of equations is obtained for kth mode

$$\begin{cases} \frac{\partial v^{(k)}}{\partial x} = -l^{(k)}\frac{\partial i^{(k)}}{\partial t} - r^{(k)}.i^{(k)} \\ \frac{\partial i^{(k)}}{\partial x} = -c^{(k)}\frac{\partial v^{(k)}}{\partial t} \end{cases} \quad k = 0, 1, 2. \tag{16}$$

$r^{(k)}$, $l^{(k)}$, and $c^{(k)}$ are modal resistance, inductance, and capacitance, respectively, and $v^{(k)}$ and $i^{(k)}$ are modal voltage and current, respectively. Equation (16) refers to a single mode and is similar in all respects to the single-phase transmission-line model. So the derivation procedure outlined previously for the symmetrical three-phase fault is applicable to each of these modal components and the solutions for other fault types can be simply derived.

III. Performance Evaluation

Since the model of the series compensator is not used in the proposed-fault location algorithm, the type and model of the series device do not affect the method, and the algorithm is applicable for all transmission lines that contain any series device. However, a 300-km, 500-kV transmission line compensated by a TCSC (shown in Fig. 1) has been chosen to evaluate the accuracy of the proposed algorithm using the Matlab/Power System Blockset simulator. The parameters of the study system are presented in Appendices A and B. The TCSC can operate in capacitive or inductive mode, although the latter is rarely used in practice. The TCSC uses voltage and current feedback for calculating its impedance. The reference impedance determines the adjusted impedance of the TCSC and a separate proportional-integral (PI) controller is utilized in each operating mode. The firing circuit uses three single-phase phase-locked loop (PLL) units for synchronization with the line current. The protection of the TCSC unit consists of an MOV in parallel with a circuit beaker, in series with a small inductor for each phase. The MOV has VI characteristics represented by a nonlinear equation. During heavy fault currents, when the absorbed energy in the MOV exceeds its limit, the TCSC transits to bypass mode.

In order to evaluate the accuracy of the presented algorithm itself, without considering the effect of the instrument transformers, the current and voltage transformers have been intentionally modeled as ideal devices.

The error of the fault location is expressed in terms of percentage of total line length as follows:

$$\%\text{Error} = \frac{\text{Calulated Distance} - \text{Actual Distance}}{\text{Line Length}} * 100. \tag{17}$$

As an example, it is assumed that the TCSC is installed 140 km from the sending end and operates in capacitive mode before the fault occurrence. A single-phase-to-ground fault occurs at 150 km from the sending end, and fault resistance is assumed to be 10 Ω. The current waveforms of the MOV, capacitor, and bypass circuit breaker are presented in Fig. 4, before and after the fault occurrence. The fault happens at t0, and during fault, the overvoltage condition is sensed by the TCSC protection; thus, the thyristor-controlled reactor (TCR) controller changes its mode to the block mode and the MOV begins to conduct at t1. This condition continues until the absorbed energy in the MOV exceeds its limit at t2. So the TCR changes its mode to bypass, and the TCSC controller sends a command to close the bypass circuit breaker.

The proposed fault-location algorithm is performed for this example. For the first stage, the values of J_R should be calculated for all m between 0 and $m_{\max R}$ for the right-hand side of the compensator. Also, in the second stage, the values of J_S should be obtained for $0 < m < m_{\max S}$. Thus, the objective function values of J_R and J_S are determined for the right- and left-hand side of the compensator, respectively, along the line and depicted in Fig. 5. The result of solving the optimization problem in stage one is $(J_R^*, x_R, R_{fR}) = (0.3874\text{e} + 006,\ 149.971\ \text{km},\ 9.995\ \Omega)$; thus, the minimum of J_R takes place at 149.97 1 km from the sending end. The obtained result from stage two is $(J_S^*, x_S, R_{fS}) = (6.6265\text{e}{+}006,\ 49.15\,\text{km},\ 53.161\,\Omega)$. So, the

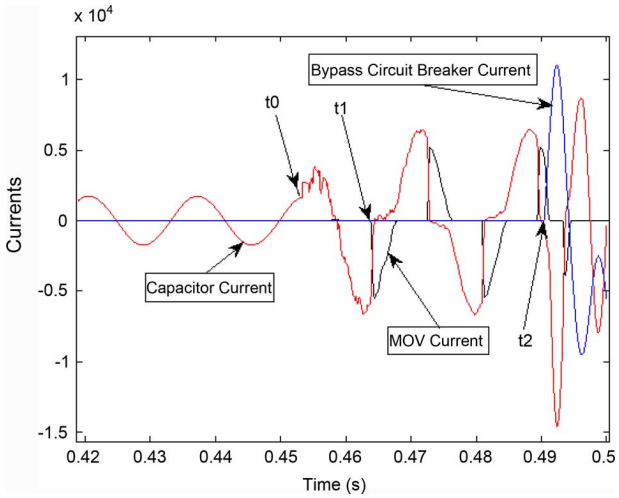

Fig. 4. Current waveforms of the MOV, capacitor, and bypass circuit breaker.

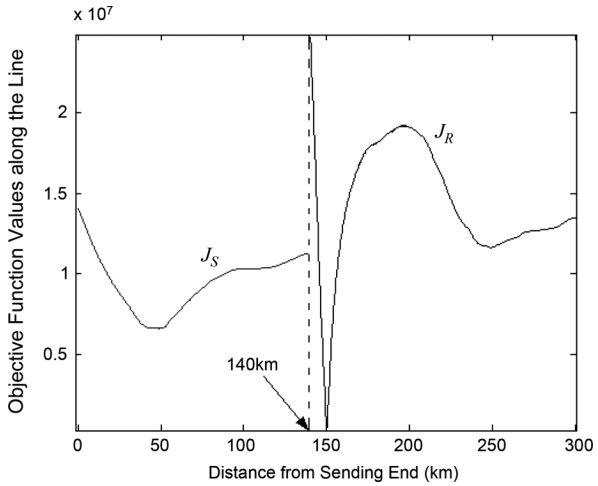

Fig. 5. Objective function values J_R and J_S along the line for a fault at 150 km from the sending end.

minimum of J_S occurs at 49.15 km from the sending end. Using (14) to select the correct solution, $J^* = J_R^* = 0.3874\text{e}+006$ is achieved and the location of fault corresponding to J_R^* is the correct one. Therefore, the fault is located at 149.971 km from the sending end and the error is -0.0096%. The proposed selector has been tested in a wide variety cases considering different fault conditions which has resulted in correct solutions in all cases.

In order to evaluate the accuracy of the proposed algorithm, several cases are considered. In the rest of this section, some of the obtained results are presented and discussed:

Case 1: Faults have occurred near boundaries: Some of the fault-location algorithms and protection methods result in errors when the fault is located near the boundaries. In this case, the proposed algorithm is tested when the faults are located near the boundaries, considering different fault resistances. The TCSC is installed at 140 km from the sending end and operates in capacitive mode. As another example, a single-line-to-ground fault occurs at 3 km from the sending end, and its resistance is assumed to be 10 Ω. The results of running stages one and two are

$$(J_R^*, x_R, R_{fR}) = (1.3205\text{e}+008,\ 264.087\,\text{km},\ 13.96\,\Omega)$$

and

$$(J_S^*, x_S, R_{fS}) = (0.218\text{e}+007,\ 3.172\,\text{km},\ 10.063\,\Omega).$$

From (14)

$$J^* = J_S^* = 0.218\text{e}+007.$$

So the fault is located 3.172 km from the sending end, and the error is 0.0574%.

The results of running the proposed algorithm for different locations of fault near the boundaries under different fault conditions are presented in Table I. In all cases, the fault inception angle is assumed to be 90°. The presented results in Table I show that the maximum absolute error is 0.0721%.

Case 2: Different fault inception angles: In order to analyze the effect of the fault inception angle on the accuracy of the proposed method, a variety of simulations has been carried out, considering different fault inception angles. Some of the results are presented in Table II. The fault resistance is assumed to be 10 Ω. The TCSC operates in capacitive mode and is installed at 140 km from the sending end. Based on the presented results in this table, it can be concluded that the accuracy of the algorithm is not sensitive to the fault inception angle. Also, it can be found that the maximum of absolute errors is 0.0792% when the fault occurs at 250 km from the sending end.

Case 3: Different locations of the TCSC: The TCSC operates in capacitive mode and is installed at different distances (80, 150, and 210 km) from the sending end. The fault resistance is assumed to be 10 Ω and the fault inception angle is 90°. The obtained results under different fault conditions are shown in Table III. It can be seen from this table that the accuracy of the algorithm is high, regardless of the location of the TCSC.

Case 4: Statistical evaluation: In this case, the proposed fault-location algorithm is evaluated with more than r 640 test cases obtained from MATLAB/Simulink for accuracy evaluation while the TCSC is installed as the same location as the case one. All of the fault-location errors are calculated for eight random locations of fault between 0–300 km, five random fault resistances between 0 Ω − 100 Ω, four random inception angles between 0°–180°, and for different types of fault (a-g, a-b, a-b-g, and a-b-c-g). The statistical results of the fault-location errors show that the maximum of absolute errors is 0.1728% when an a-g fault occurs at 268 km from the sending end, and the fault resistance is large. The average of absolute errors is about 0.0625%.

According to the entries of Tables I–III and the statistical evaluation, it can be seen that the proposed algorithm is very precise and insensitive to the value of the fault resistance, fault inception angle, location of fault, fault type, and location of compensator.

TABLE I
RESULTS OF RUNNING THE PROPOSED ALGORITHM CONSIDERING NEAR BOUNDARY FAULTS

Fault type	Actual location of fault (km)	R_f=1Ω		R_f=10Ω		R_f=100Ω	
		Calculated location of fault (km)	Error (%)	Calculated location of fault (km)	Error (%)	Calculated location of fault (km)	Error (%)
Single-phase to ground	3	3.172	0.0574	3.172	0.0574	3.172	0.0574
	136	136.12	0.0408	136.12	0.0408	136.12	0.0408
	143	143.047	0.0156	143.047	0.0156	143.047	0.0156
	296	295.939	-0.0202	295.939	-0.0202	296.216	0.0721
Three-phase to ground	3	2.924	-0.0253	2.924	-0.0253	2.924	-0.0253
	136	135.874	-0.0420	135.874	-0.0420	136.151	0.0503
	143	143.047	0.0156	143.047	0.0156	143.047	0.0156
	296	296.216	0.0721	296.216	0.0721	296.216	0.0721
Double-phase to ground	3	3.172	0.0574	3.172	0.0574	3.172	0.0574
	136	136.122	0.0408	136.122	0.0408	136.122	0.0408
	143	143.047	0.0156	143.047	0.0156	143.047	0.0156
	296	295.939	-0.0202	296.216	0.0721	296.216	0.0721
Double-phase	3	3.172	0.0574	3.172	0.0574	3.172	0.0574
	136	136.122	0.0408	136.122	0.0408	136.122	0.0408
	143	143.047	0.0156	143.047	0.0156	143.047	0.0156
	296	296.216	0.0721	296.216	0.0721	296.216	0.0721

TABLE II
RESULTS OF RUNNING THE PROPOSED ALGORITHM WITH RESPECT TO DIFFERENT FAULT INCEPTION ANGLES

Fault type	Actual location of fault (km)	Fault inception angle=0°		Fault inception angle=45°		Fault inception angle=90°	
		Calculated location of fault (km)	Error (%)	Calculated location of fault (km)	Error (%)	Calculated location of fault (km)	Error (%)
Single-phase to ground	100	100.115	0.0383	100.115	0.0383	100.115	0.0383
	250	249.96	-0.0131	249.96	-0.0131	249.96	-0.0131
Three-phase to ground	100	100.115	0.0383	100.115	0.0383	100.115	0.0383
	250	250.238	0.0792	250.238	0.0792	250.238	0.0792
Double-phase to ground	100	100.115	0.0383	100.115	0.0383	100.115	0.0383
	250	249.96	-0.0131	250.238	0.0792	250.238	0.0792
Double-phase	100	100.115	0.0383	100.115	0.0383	100.115	0.0383
	250	250.238	0.0792	250.238	0.0792	250.238	0.0792

Case 5: Effect of mis-synchronization of the gathered signals: This paper proposes a new approach, considering synchronous measurement data gathered from both ends of the transmission line. However, in order to study the effect of synchronization error of the gathered data from two ends of the line on the accuracy of the fault-location estimation, simulation examples with respect to different fault resistances and various fault locations have been performed. A synchronization error of −15, −10, 10, and 15° has been added to the measurements at terminal S and some of the results are shown in Table IV. It can be concluded that the accuracy of the algorithm is high for low fault resistances. When the fault resistance is 30 Ω and the synchronization error is 15°, it will cause up to a 1.9258% error in the fault location, while the fault occurs 250 km from the sending end. For larger fault resistances, it has been found that the fault-location errors increased.

Case 6: Effect of measurement errors: In practice, conventional instrument transformers (i.e., current transformers (CTs) and capacitor voltage transformers (CVTs)) may insert errors in measurements. For comprehensive evaluation, two approaches are considered to study the effect of measurement errors on the accuracy of the proposed method. In the first approach, to consider the effect of distorted signals, the gathered samples from both ends of the transmission line are subjected to random perturbations, and then are fed into the presented method. In the second approach, to study the effect of frequency responses of the CTs and CVTs, these instruments are modeled and these models are used in simulations. These two approaches are explained as follows.

- *Effect of noise in the measurements*: The TCSC is installed at 140 km from the sending end, and the fault resistance is considered to be 10 Ω. To study the influence of the measurement errors on the accuracy of the proposed algorithm for different locations of fault, the voltage and current samples obtained from Matlab/Simulink are subjected to perturbations. Thus, errors

TABLE III
RESULTS OF RUNNING THE PROPOSED ALGORITHM WITH RESPECT TO DIFFERENT LOCATION OF TCSC

Fault type	Actual location of fault (km)	TCSC is installed at 80km from the sending end		TCSC is installed at 150km from the sending end		TCSC is installed at 210km from the sending end	
		Calculated location of fault (km)	Error (%)	Calculated location of fault (km)	Error (%)	Calculated location of fault (km)	Error (%)
Single-phase to ground	50	49.809	-0.0636	50.011	0.0035	50.183	0.0610
	240	239.817	-0.0610	240.018	0.0061	239.914	-0.0287
Three-phase to ground	50	50.086	0.0287	50.011	0.0035	49.906	-0.0313
	240	240.094	0.0313	240.018	0.0061	239.914	-0.0287
Double-phase to ground	50	49.809	-0.0636	49.809	-0.0636	49.906	-0.0313
	240	239.817	-0.0610	239.817	-0.0610	239.914	-0.0287
Double-phase	50	49.809	-0.0636	49.809	-0.0636	49.906	-0.0313
	240	239.817	-0.0610	239.817	-0.0610	239.914	-0.0287

TABLE IV
EFFECT OF SYNCHRONIZATION ERRORS ON THE ACCURACY OF THE PROPOSED METHOD

Actual location of fault (km)	Fault Resistance (Ω)	Synch. error= -15°	Synch. error= -10°	Synch. error= 10°	Synch. error= 15°
		Fault location error (%)			
100	1	-0.1463	-0.1463	-0.1463	0.0383
	10	-0.3310	-0.1463	0.0383	0.2230
	30	-1.0696	-0.5156	0.7769	1.1462
250	1	0.0792	0.0792	0.0792	0.0792
	10	-0.2901	-0.1054	0.2639	0.2639
	30	-1.5826	-1.2133	1.1872	1.9258

TABLE V
RESULTS OF RUNNING THE PROPOSED ALGORITHM IN THE PRESENCE OF NOISE IN THE MEASUREMENTS

Fault type	Actual location of fault (km)	Calculated location of fault (km)	Error (%)
Single-phase to ground	40	39.733	-0.0888
	130	129.474	-0.1751
	190	190.964	0.3214
	275	275.719	0.2399
Three-phase to ground	40	39.733	-0.0888
	130	130.028	0.0096
	190	189.856	-0.0479
	275	275.165	0.0553
Double-phase to ground	40	39.733	-0.0888
	130	130.028	0.0096
	190	189.856	-0.0479
	275	275.165	0.0553
Double-phase	40	39.733	-0.0888
	130	130.028	0.0096
	190	189.856	-0.0479
	275	275.165	0.0553

are generated randomly between −2.5% and +2.5% for each measured voltage and current samples of buses S and R and then are fed into the new fault-location algorithm. The obtained results of the fault location are depicted in Table V for different locations of the fault. The maximum absolute error is 0.3214% while single-phase-to-ground fault occurs at 190 km from the sending end. The executed tests have shown that the obtained fault-location errors are small, and the accuracy of the proposed method is high.

TABLE VI
RESULTS OF RUNNING THE PROPOSED ALGORITHM CONSIDERING FREQUENCY RESPONSES OF CTS AND CVTS

Fault type	Actual location of fault (km)	R_f=1Ω	R_f=10Ω	R_f=100Ω
		Fault location error (%)		
Single-phase to ground	40	0.0958	-0.0888	-0.2735
	130	0.3789	0.3789	-0.1751
	190	-0.0479	-0.0479	1.9833
	275	0.0553	0.0553	0.6092
Three-phase to ground	40	0.0958	-0.0888	-0.4581
	130	2.2254	0.1942	-0.5444
	190	0.5060	-0.0479	-3.0024
	275	0.0553	0.0553	3.5637
Double-phase to ground	40	0.0958	-0.0888	-0.4581
	130	0.5635	0.1942	-0.3597
	190	0.6907	-0.0479	-2.0791
	275	0.0553	0.2399	0.6092
Double-phase	40	0.0958	0.0958	-0.2735
	130	0.3789	0.3789	-0.5444
	190	1.2447	-0.2326	0.5060
	275	0.0553	0.0553	0.7939

- *Effect of frequency responses of CTs and CVTs:* To consider the effect of frequency responses of CTs and CVTs on the accuracy of the proposed method, the chosen model of instrument transformers employed for the simulations should include features that accurately represent their characteristics. Thus, simulations have been performed using detailed models of saturable current and voltage transformers to evaluate the impact of CTs and CVTs on the accuracy of the fault-location algorithm (details of the employed models and parameters can be found in [10]). The obtained results are presented in Table VI for different fault conditions. Based on the shown results in this table, it can be seen that the maximum fault-location error is kept bellow 3.6%.

The presented algorithm is also evaluated in the following cases:

- when the prefault power-flow direction was reversed by changing the voltage phase angle between the sending and receiving ends;
- while the parameters of the controller system are changed; the parameters contain: PI controller parameters, references, MOV energy threshold, and MOV protection level;
- when Thevenins' equivalents of the external networks are varied;
- while the parameters of the transmission line (including positive-, negative-, and zero-sequence parameters) are changed.

To save space, a detailed evaluation of the proposed algorithm is not presented for these four cases. However, the executed tests have shown that the accuracy of the fault-location method is high and similar to that presented previously.

IV. Conclusion

In this paper, a new and accurate noniterative fault-location algorithm for long transmission lines compensated by series FACTS devices is proposed. There are difficulties in the modeling the series FACTS devices during fault. In order to overcome this problem, the proposed technique does not use the model of the series device and it can be easily applied to any transmission line that contains any series device where its input current is equal to the output current. In addition, the proposed fault-location algorithm does not need iterative calculations. Since the fault position with respect to the series compensator is not known prior to fault-location estimation, the proposed algorithm considers two fault points in stages 1 and 2, the fault on the right-hand side of the series compensator, and the fault on the left-hand side of it. Applying these stages, two solutions are obtained for the fault location. Then, in stage 3, a comparing selector has been proposed to select the correct solution, and the objective function values obtained from the first two stages are compared, and the correct fault location is concluded. The simulation results show that the accuracy of the proposed fault-location algorithm is high.

Appendix A
Transmission Line

Zero sequence

$$R_0 = 0.275\ \left(\frac{\Omega}{\mathrm{km}}\right)$$
$$L_0 = 3.4505998\ \left(\frac{\mathrm{mH}}{\mathrm{km}}\right)$$
$$C_0 = 8.5\ \left(\frac{\mathrm{nF}}{\mathrm{km}}\right).$$

Positive sequence

$$R_1 = 0.0275\ \left(\frac{\Omega}{\mathrm{km}}\right)$$
$$L_1 = 1.00268\ \left(\frac{\mathrm{mH}}{\mathrm{km}}\right)$$
$$C_1 = 13\ \left(\frac{\mathrm{nF}}{\mathrm{km}}\right).$$

Appendix B
TCSC

TCR inductance: 43 (mH)
TCSC capacitance $31.18(\mu\mathrm{F})$.

References

[1] M. M. Saha, I. Izykowski, E. Rosolowski, and B. Kasztenny, "A new accurate fault locating algorithm for series compensated lines," *IEEE Trans. Power Del.*, vol. 14, no. 3, pp. 789–797, Jul. 1999.

[2] D. Novosel, B. Bachmann, D. Hart, Y. Hu, and M. M. Saha, "Algorithms for locating faults on series compensated lines using neural network and deterministic methods," *IEEE Trans. Power Del.*, vol. 11, no. 4, pp. 1728–1736, Oct. 1996.

[3] J. Sadeh, N. Hadjsaid, A. M. Ranjbar, and R. Feuillet, "Accurate fault location for series compensated transmission lines," *IEEE Trans. Power Del.*, vol. 15, no. 3, pp. 1027–1033, Jul. 2000.

[4] M. Al-Dabbagh and S. K. Kapuduwage, "Using instantaneous values for estimating fault locations on series compensated transmission lines," *Elect. Power Syst. Res.*, vol. 76, pp. 25–32, 2005.

[5] C.-S. Yu, C.-W. Liu, S.-L. Yu, and J.-A. Jiang, "A new PMU based fault location algorithm for series compensated lines," *IEEE Trans. Power Del.*, vol. 17, no. 1, pp. 33–46, Jan. 2002.

[6] J. Sadeh and A. Adinehzadeh, "Accurate fault location algorithm for transmission line in the presence of series connected FACTS devices," *Int. J. Elect. Power Energy Syst.*, vol. 32, no. 4, pp. 323–328, May 2010.

[7] M. Khederzadeh and T. S. Sidhu, "Impact of TCSC on the protection of transmission lines," *IEEE Trans. Power Del.*, vol. 21, no. 1, pp. 80–87, Jan. 2006.

[8] J. Izykowski, E. Rosolowski, P. Balcerek, M. Fulczyk, and M. M. Saha, "Accurate noniterative fault location algorithm utilizing two-end unsynchronized measurements," *IEEE Trans. Power Del.*, vol. 25, no. 1, pp. 72–80, Jan. 2010.

[9] A. T. Johns and S. K. Salman, *Digital Protection for Power Systems*. London, U.K.: Peregrinus, 1995.

[10] M. Kezunovic, A. Abur, Lj. Kojovic, V. Skendzic, and H. Singh, "DYNA-TEST simulator for relay testing, Part II: Performance evaluation," *IEEE Trans. Power Del.*, vol. 7, no. 3, pp. 1097–1103, Jul. 1992.

Mahdi Ghazizadeh Ahsaee was born in Kerman, Iran, in 1977. He received the B.Sc. degree in electronic engineering from Bahonar University of Kerman, Kerman, Iran, in 2000, the M.Sc. degree in electrical engineering from Mazandaran University, Babol, Iran, in 2003, and is currently pursuing the Ph.D. degree at the Ferdowsi University of Mashhad, Mashhad, Iran.

He was a Scientific Member at the University of Zabol, Zabol, Iran. His research interests are power system protection, fault location, and operation.

Javad Sadeh (M'08) was born in Mashhad, Iran, in 1968. He received the B.Sc. and M.Sc. degrees in electrical engineering (Hons.) from Ferdowsi University of Mashhad, Mashhad, Iran, in 1990 and 1994, respectively, and the Ph.D. degree in electrical engineering from Sharif University of Technology, Tehran, Iran, with the collaboration of the electrical engineering laboratory of the Institut National Polytechnique de Grenoble (INPG), Grenoble, France, in 2001.

Currently, he is an Associate Professor in the Department of Electrical Engineering, Ferdowsi University of Mashhad. His research interests are power system protection, dynamics, and operation.